

Effects of surfactants on Faraday-wave dynamics

By DIANE M. HENDERSON

Department of Mathematics, Pennsylvania State University, University Park, PA 16802, USA

(Received 25 September 1995 and in revised form 2 January 1998)

The damping rates, natural frequencies and amplitudes of parametrically excited, standing, water waves in a partially filled, right circular cylinder are measured and compared to existing theoretical models that assume wave slopes are small. The water surfaces were covered by insoluble monomolecular (surfactant) films of oleyl alcohol, lecithin, diolein, cholesterol, and arachidyl alcohol whose concentrations were varied from zero (clean) to saturation; wave slopes were varied from about 0.1 to 1.2. Measured damping rates increased with increasing film concentration as predicted using films of oleyl alcohol, lecithin, and diolein, even when wave slopes were about one. Measured damping rates increased with increasing film concentration as predicted, using films of cholesterol and arachidyl alcohol when wave slopes were small, but not when wave slopes were large. In fact, the measured damping rates for large-slope waves on these films were equivalent to those of waves on a clean surface. Measured natural frequencies varied as predicted for all films, but were about 5% larger. Contact-line effects are incorporated, using an empirical value for contact-line speed, to account for discrepancies between measurements and predictions of damping rates and natural frequencies. Measured steady-state amplitudes agreed well with predictions that used measured damping rates and natural frequencies in the calculations for all films except lecithin and arachidyl alcohol for which there was significant disagreement.

1. Introduction

In this paper, we examine experimentally and theoretically the effects of insoluble surfactants on the damping rates, natural frequencies and amplitudes of the fundamental, axisymmetric, Faraday, wave mode in circular cylinders with radii of 2.77 cm. Faraday waves are subharmonic standing waves that are excited parametrically by vertical oscillations of a fluid (e.g. see Miles & Henderson (1990) for a review). Our purpose is to (i) determine the effects of elastic, insoluble films on Faraday wave dynamics, and (ii) examines the effects of films on the damping rates of large-amplitude, low-frequency (about 6 Hz) waves in general. For (ii), the advantages of Faraday waves over the progressive waves used in previous investigations are that (i) measurements of the damping rates of standing waves are temporal and simpler than the spatial measurements required of progressive waves, (ii) the surfactant is spread over a small surface area, (iii) lower-frequency, large-amplitude waves are possible, and (iv) the waves are not subject to amplitude changes due to nonlinear instabilities of deep-water, progressive waves (e.g. see Hammack & Henderson 1993). In particular, deep-water, progressive waves in the frequency range 1–6.9 Hz and 9.8–19.6 Hz are unstable to transverse modulations as predicted by a nonlinear Shroedinger equation (Perlin & Hammack 1991); waves with frequencies from 6.9–9.8 Hz are unstable to superharmonics known as Wilton ripples (Perlin & Ting 1992); and waves with frequencies greater than 19.6 Hz are unstable to resonant triad interactions (Perlin,

Henderson & Hammack 1990). These instabilities cause a decrease in energy that may be mistaken for viscous damping. The disadvantage of the Faraday-wave system is that we cannot determine quantitatively the possible contribution of the dynamic contact line. The effects of various static contact angles were discussed by Henderson *et al.* (1992).

To this end we measured damping rates, natural frequencies and wave amplitudes of the fundamental, axisymmetric mode at an air–water interface that was clean or covered with varying concentrations of the insoluble surfactants diolein, arachidyl alcohol, oleyl alcohol, cholesterol, and lecithin. We compared damping rates and natural frequencies to predictions from Miles' (1967) theory for the damping of waves in closed basins owing to viscoelastic films. Agreement between measured and predicted damping rates was reasonable even for large-amplitude waves (wave slopes approaching one) using surfactants made of oleyl alcohol, lecithin, and diolein. Cholesterol and arachidyl alcohol did increase damping rates as expected when the wave amplitudes were small; however, when wave amplitudes were large, the waves damped as if the surface was clean, even when it was saturated with one of these films. The measured natural frequencies were larger than predicted. Contact-line effects are incorporated using Miles' (1991) results with empirical values of contact-line speed to account for discrepancies between predictions and measurements of damping rates and natural frequencies. Amplitudes of waves as a function of film concentration were in reasonable agreement with predictions for all films except lecithin and arachidyl alcohol if the measured damping rates and measured natural frequencies were used in the calculations. Amplitudes of waves on lecithin and arachidyl alcohol did not change with increasing film concentration, in disagreement with predictions.

The enhanced damping of waves owing to surfactants at an air–water interface has been known since antiquity. The large damping rates result from flows induced by spatial gradients in surface tension that arise when a film is compressed and expanded by wave action (see for example Miles (1967) for a review). Lucassen-Reynders & Lucassen (1969) provide a review of surfactant rheology and its characterization for applications to the hydrodynamic theory of water waves. Alpers & Huhnerfuss (1989) provide a review of geophysical observations of wave damping due to films. Typically, the primary property of a film that accounts for its effect on wave damping is its elasticity. Film elasticity is related to the variation of surface pressure π (defined as the difference between the surface tension values of the surface with and without surfactants) as a function of the surfactant (area) concentration Γ . When the surfactant concentration of a monolayer is saturated, π is maximum and remains constant with further addition of surfactant. The slope of the (π, Γ) -relationship is proportional to the elasticity of the film and must be measured to obtain the coefficient of elasticity of the film. Lamb's (1945, §351) wave-damping model for an inextensible surface, i.e. one that neither compresses nor expands, corresponds to a film for which the slope of the (π, Γ) -curve, and correspondingly the elasticity, is infinite. Wave-damping models that include finite (non-zero) elasticity predict that the damping rates depend on surfactant concentration and that the maximum rate may be as much as twice that predicted for inextensible films. Experimental measurements, such as those of Davies & Vose (1965) and Lucassen & Hansen (1965), have verified this prediction for high-frequency, small-amplitude, progressive waves on deep water. Moreover, this enhanced wave damping by films with finite elasticity has also been found to depend on wave frequency. For example, Cini & Lombardini's theory (1978) and experiments (1981) showed damping rates of twice the inextensible value at a particular frequency. They concluded that this maximum damping occurred in consequence of a resonance between the transverse

water-wave and the longitudinal (elastic) Marangoni wave of the film. They observed this peak experimentally for both progressing and standing waves with frequencies from about 4–15 Hz. Huhnerfuss, Lange, & Walter (1985*a*) reported experiments on progressing waves with frequencies 1–2.5 Hz and showed that the relaxation of the surfactant molecules during wave passage causes a phase shift between the wave and the film dynamics. This phase shift can be parameterized as a ‘dynamical’ surface elasticity that is much greater than that determined by static measurements of the (π, Γ) -relationship. Huhnerfuss *et al.* (1985*b*) showed that this dynamical surface elasticity can cause an additional increase in damping that is as large as the enhancement caused by finite (static) film elasticity. Bock (1987) measured the damping rates of progressive waves with frequencies from 4 to 20 Hz on viscous fluids with and without films added. He found reasonable agreement between measurements and predictions from classical theory when the surface was clean, and observed a large jump in the damping rate when a surfactant was added. Bock & Mann (1989) re-examined the dispersion of gravity–capillary waves due to surface elasticity. They solved the dispersion relation numerically to obtain gravity–capillary waves travelling in opposite directions as well as Marangoni modes. Bock (1989) observed dispersion of gravity–capillary wave packets on fluids with soluble and insoluble surfactants.

A brief outline of the paper is as follows. Section 2 presents the weakly nonlinear theory for wave amplitudes of Faraday waves from Miles (1984) and predictions of the damping coefficients for standing waves from Miles (1967) that incorporate damping due to the elasticity of the surface film as well as the contribution to damping from Stoke’s-type boundary layers at the rigid boundaries. Contact-line effects are considered from Miles (1991). The experimental apparatus is described in §3. Measurements of damping rates, amplitudes and natural frequencies are compared to predictions in §4. A list of conclusions is provided in §5.

2. Theory

Figure 1 is a schematic of the circular cylinders and fundamental axisymmetric wave mode. The motion of the inviscid, irrotational fluid in the circular cylinder is described by the well-known (Lamb 1945) boundary-value problem for waves in closed basins. Herein, we posit the normal-mode solutions to this problem, predictions of wave amplitudes from a weakly nonlinear theory for single-mode Faraday waves (Miles 1984) and the damping coefficients from Miles (1967). We note that the experiments are tuned so that only one mode is available for excitation; i.e. there are no other modes available with nearby or integer multiple natural frequencies. Thus, the theory presented here is for the excitation of a single mode.

The linearized, unforced solution for the free surface displacement is

$$\eta = a[p \cos \omega_{lm} t + q \sin \omega_{lm} t] J_m(k_{lm} r) \cos m\psi, \quad (1)$$

where the wavenumber, k_{lm} , of the (l, m) mode depends on the radius, R , of the cylinder and is obtained from

$$J'_m(k_{lm} R) = 0. \quad (2a)$$

The wavenumber is related to the natural frequency, ω_{lm} , by the dispersion relation

$$\omega_{lm} = [(gk_{lm} + Tk_{lm}^3) \tanh k_{lm} h]^{1/2}, \quad (2b)$$

where g is the acceleration due to gravity and T is the kinematic coefficient of surface tension. If the forcing is non-zero, then the shape of the waves that grow is

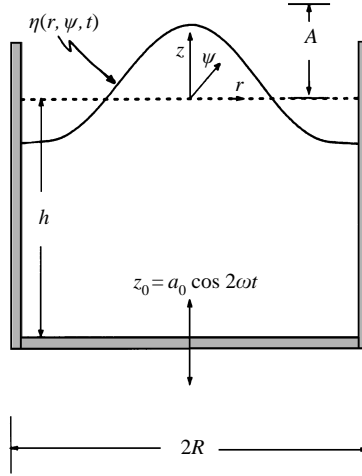


FIGURE 1. Schematic drawing of the (0, 1) mode in a circular cylinder.

approximated by (1), but have frequencies equal to ω , which is half the forcing frequency rather than the natural frequency. The amplitude is a function of slow time $\tau = \epsilon\omega t$ where $\epsilon = a_0 k_{lm} \tanh k_{lm} h \ll 1$ is the dimensionless forcing parameter, and a_0 is the dimensional forcing amplitude. The evolution equations for the amplitudes were given by Miles (1984) and can be written in terms of dimensional time as

$$\frac{dp}{dt} + \gamma p = -\epsilon\omega q[\beta - 1 + (p^2 + q^2)], \quad (3a)$$

$$\frac{dq}{dt} + \gamma q = \epsilon\omega p[\beta + 1 + (p^2 + q^2)], \quad (3b)$$

where p and q are dimensionless, slowly varying amplitudes, and the lengthscale a from (1) is given by Miles (1984). (See Henderson & Miles (1990) for an application of the theory to previous experiments.) Weak viscous effects have been incorporated into (3) through the linear damping rate, γ , which is discussed below. The tuning parameter,

$$\beta = \frac{\omega^2 - \tilde{\omega}_{lm}^2}{2\epsilon\omega^2} = \frac{\Delta}{\epsilon\omega}, \quad (4)$$

describes how close the forced wave frequency is to the natural frequency. (Here, $\tilde{\omega}_{lm}$ is the actual natural frequency of the wave, which may or may not agree with the inviscid value from (2b), the viscous value from (13), or the viscous value that also includes contact line effects from (16).) When the forcing is turned off, ($\epsilon = 0$), (3a) and (3b) are trivially solved for p and q so that the surface displacement becomes

$$\eta = e^{-\gamma t} [p_0 \cos(\omega - \Delta)t + q_0 \sin(\omega - \Delta)t] J_m(k_{lm} r) \cos m\psi, \quad (5)$$

where p_0 and q_0 are the steady-state amplitudes during forcing.

If we consider the effects of viscosity in the fluid to be confined to thin boundary layers about the wetted surfaces of the cylinder and at the air–water interface, then a boundary-layer analysis provides estimates of the linear damping rate γ . Thus, the linear damping rate is

$$\gamma = \gamma_b + \gamma_{sw} + \gamma_s, \quad (6)$$

where γ_b is the contribution from the bottom boundary layer, γ_{sw} is the contribution from the sidewall boundary layer, and γ_s is the contribution from the air–water interface. The solid boundaries behave like Stokes boundary layers with damping rates of

$$\gamma_b = \frac{\delta\omega_{lm}}{2 \sinh(2k_{lm}h)}, \quad (7)$$

and

$$\gamma_{sw} = \frac{\delta\omega_{lm}}{4k_{lm}R} \left[\frac{1 + \frac{l^2}{k_{lm}R}}{1 - \frac{l^2}{k_{lm}R}} - \frac{2k_{lm}h}{\sinh 2k_{lm}h} \right], \quad (8)$$

where $\delta = k_{lm}(2\nu/\omega_{lm})^{1/2} \ll 1$ is the boundary-layer thickness, non-dimensionalized by k_{lm} . When the air–water interface is covered by an insoluble surfactant with negligible shear and dilational viscosities, the damping rate due to the surface as given by Miles (1967) is

$$\gamma_s = \frac{1}{4}\delta\omega_{lm} \frac{\xi^2}{(\xi-1)^2+1} \coth k_{lm}h, \quad (9)$$

where

$$\xi = \rho^{-1}(\nu\omega_{lm}^3/2)^{-1/2}k_{lm}^2\Gamma_0 \frac{d\pi}{d\Gamma_0} \quad (10)$$

is the non-dimensional elasticity of the surface film. Here, Γ_0 is the surfactant concentration of the quiescent surface, and π is the surface pressure. If the film is rigid, so that the elasticity becomes infinite, then γ_s reduces to the result given by Lamb (1945) for damping of waves on an inextensible surface, i.e.

$$\gamma_s^{in} = \frac{1}{4}\delta\omega_{lm} \coth k_{lm}h. \quad (11)$$

If the surface is pure, so that there is no film, then γ_s approaches zero, and the contribution to damping from the surface is second order in δ and equal to

$$\gamma_s^{pure} = \delta^2\omega_{lm}. \quad (12)$$

The boundary layers along the bottom and lateral boundaries decrease the natural frequencies of the standing wave modes by a few per cent. The effect of the surface film can be either to increase or decrease the natural frequency, depending on the elasticity of the surface. Thus, the natural frequency of the standing wave modes that takes into account viscous effects confined to the wetted perimeters of the boundaries is

$$\hat{\omega}_{lm} = \omega_{lm} - \gamma_b - \gamma_{sw} - \gamma_e, \quad (13)$$

where

$$\gamma_e = \frac{1}{4}\delta\omega_{lm} \frac{\xi^2 - 2\xi}{(\xi-1)^2+1} \coth k_{lm}h$$

is the contribution from an elastic surface and ω_{lm} is given by (2b). In §4 (figure 3), (11) is used in (6) and replaces γ_e in (13) when the surface is saturated; i.e. when $d\pi/d\Gamma_0 = 0$.

The dynamics of the contact line also increase damping and affect the natural frequencies of the waves (see Ting & Perlin (1995) for a review). To include damping due to contact line effects, Hocking (1987) replaced the classic requirement on the

lateral boundary that $\hat{\mathbf{n}} \cdot \nabla \eta = 0$, where $\hat{\mathbf{n}}$ is the inwardly directed normal to the lateral boundary, by $c\hat{\mathbf{n}} \cdot \nabla \eta = i\omega\eta$ where c is the real-valued speed of the contact line. Miles (1991) allowed c to be complex to allow for the effects of the contact line both on wave damping and on the natural frequency of the wave. His analysis results in a natural frequency $\hat{\omega}_{lm}$ corrected by contact line effects, such that,

$$\frac{\hat{\omega}_{lm}^2 - \omega_{lm}^2}{\omega_{lm}^2} = \frac{F_{lm}}{1 - i\lambda} [1 + O(k_{lm} l_c)], \quad (14)$$

where $l_c = (T/g)^{1/2}$ is the capillary length,

$$F_{lm} = \frac{2k_{lm}^2 R l_c}{k_{lm}^2 R^2 - m^2} \quad (15)$$

is a form factor, and $\lambda = c/\omega l_c$ is the normalized (where ω is the radian frequency of the free surface oscillations), complex, contact-line speed with $\text{Re}(\lambda) > 0$. Herein, the maximum value of $k_{lm} l_c = 0.37$ occurs when the surface is clean, so that (14) is applicable here. To apply Miles' theory, we let $\lambda = \lambda_R + i\lambda_I$. The maximum value of F_{lm} is 0.20 (herein, $m = 0$). Thus (14) can be approximated as

$$\hat{\omega}_{lm} \approx \omega_{lm} \left[1 + \frac{1}{2} F_{lm} \frac{(1 + \lambda_I)}{(1 + \lambda_I)^2 + \lambda_R^2} + i\omega_{lm} \frac{F_{lm}}{2} \frac{\lambda_R}{(1 + \lambda_R)^2 + \lambda_I^2} \right]. \quad (16)$$

The real part of (16) causes a change in the natural frequency; the imaginary part causes a change in the damping rate.

3. Experimental apparatus and procedures

The experimental apparatus comprised glass circular cylinders, a computer system, an electromagnetic shaker with feedback, an *in situ* wave gauge and various insoluble surfactants. The cylinders were crystallizing dishes made of annealed glass with radii of $R = 2.77 \pm 0.01$ cm. We found that annealed glass provided for a smooth contact line that had a contact angle of nearly 90° when the water was quiescent. Neither the smoothness of the contact line nor the value of the contact angle was consistent when standard, Pyrex cylinders were used. The cylinders were cleaned by rinses in chromic acid, tap water, distilled water, and acetone, and then heated at 80°C . (The acetone was from Fisher Scientific and was 99.5% pure.) A different cylinder was used for each experiment. Doubly distilled water was filtered through Whatman paper to remove particles larger than $11\ \mu\text{m}$ and added to a cylinder. The surface was vacuumed with a pipette until the depth was $h = 2.00 \pm 0.02$ cm. The surface tension was measured (accurate to $0.5\ \text{dyn cm}^{-1}$) with a Wilhelmy plate connected to a Statham transducer readout. The (0, 1) mode was excited on the clean surface, and its damping rate was measured as described below. Then, a known amount of surfactant was applied to the surface with an Agla microsyringe (Burroughs–Wellcome), and the surface tension was again measured, relative to the previous clean surface value.

An electrodynamic shaker, Bruel & Kjaer minishaker Type 4810, oscillated the cylinder vertically. A non-contacting proximity sensor (Kaman Model KD-2310) monitored the shaker motion and provided a signal to a servocontroller. The controller acted as a feedback device to ensure that the actual motion followed the programmed

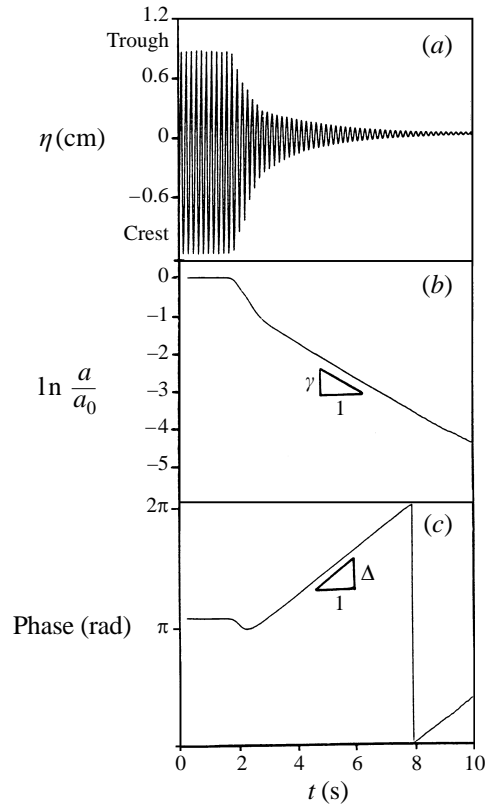


FIGURE 2. Results of complex-demodulation, (a) raw time series; (b) natural log of the amplitude normalized by the steady-state amplitude; (c) phase.

one; additionally, it provided measurements of the forcing amplitude, accurate to 0.005 mm. For all experiments, the forcing amplitude was 0.43 mm except when discussed otherwise. The command signal to the shaker was provided by a MicroVAX Workstation II, which had analog input and output systems with two separate, programmable real-time clocks.

The surface displacement was measured with an *in situ*, glass, capacitance-type gauge with a diameter of 1.15 mm (the wavelength of the (0, 1) mode was 21.7 mm). The gauge signal was low-pass-filtered twice at 30 Hz by a Kronhite Model 3323 analog filter, which also produced a 20 dB gain. It was then digitized at 350 Hz by the computer. The gauge was calibrated by comparing its signal to mechanical measurements of surface displacement with a Lory Type C point gauge combined with a dial micrometer accurate to 0.01 mm. The wave amplitudes quoted in §3 and 4 were measured with an accuracy of 0.01 mm and are half the total displacement of the surface in one wave period.

To determine damping rates, first we measured the time series of the water surface displacement before and after the shaker was turned off. Second, we complex-demodulated the time series at half the forcing frequency to obtain the amplitude and phase of the surface displacement averaged over 100 points (or 0.35 s). Figure 2 shows a time series and the complex-demodulated amplitudes and phases for a typical experiment. The amplitudes in figure 2(b) are shown on a log scale; thus the slope of the curve is the damping rate, which is accurate to $\pm 0.01 \text{ rad s}^{-1}$. The phase of the

wave, shown in figure 2(c) provides a measure of the actual wave frequency, accurate to 10^{-6} Hz. The horizontal line from about $t = 0$ to $t = 1.8$ indicates that while forced, the wave had a frequency equal to half that of the forcing. After the forcing was discontinued, the wave frequency changed by an amount Δ , which is related to the difference between the natural and forced frequencies. Thus, the natural frequencies of the waves were computed from (4) and measurements of Δ . (For a check on this method of measuring natural frequencies, we compared values obtained from this procedure to values obtained by measuring the peak of the amplitude versus frequency curve for the horizontally excited fundamental mode.)

Calculations of theoretical damping rates using (10) require knowledge of the gradient of surface pressure, π , with surfactant concentration, Γ . Herein, this gradient was determined indirectly by measuring the (π, Γ_0) -curve and empirically fitting either a power law or linear relationship between the two. In §4 the (π, Γ_0) -curve for each surfactant is shown, as well as the fitted relationship. (The subscript 0 indicates the surfactant concentration of the quiescent surface.)

The insoluble surfactants used in this investigation were diolein, a 1.9×10^{-3} molar solution of oleyl alcohol, 2.0×10^{-3} , 3.3×10^{-3} and 6.7×10^{-3} molar solutions of lecithin, a 1.0 molar solution of arachidyl alcohol, and a 1.5×10^{-3} molar solution of cholesterol. The arachidyl alcohol, cholesterol and lecithin surfactants were chosen to consider whether there is an effect on wave damping owing to the solid or liquid state of the film. Arachidyl alcohol creates a solid-like film, while lecithin and cholesterol create liquid-like films. Mixing cholesterol with arachidyl alcohol acts to liquify the solid film created by the alcohol, while mixing it with lecithin acts to solidify the liquid film created by lecithin. The remaining surfactants create liquid films. Two differences between the solid and liquid states of a film are manifest in (1) the surface pressure *vs.* concentration (π, Γ_0) -curve; and (2) properties of evaporation of the water-substrate. A solid-like film is characterized by a large gradient in the (π, Γ) -curve, whereas a liquid curve has a smaller gradient. Evaporation of the substrate fluid is negligible through a solid film, but significant through a liquid film (Rao & Shah 1990).

4. Results

Herein we present the experimental results for surface pressure (§4.1), wave damping (§4.2), and natural frequencies, (§4.3) and discuss them within the framework of the linear theory presented in §2. Contact-line effects are incorporated in the predictions of damping rates and natural frequencies in §4.4 as a likely explanation for discrepancies between measurements and predictions. All of these results are shown in figure 3. In §4.5 we present measurements of wave amplitudes as well as results that do not appear to be described by the linear theory.

4.1. Surface pressure

To compute values for predicted damping rates and natural frequencies, we must first obtain the gradient of surface pressure with respect to surfactant concentration. Figure 3 shows measurements of surface pressures (figure 3*c*, *f*, and *i*), damping rates, and natural frequencies as a function of surfactant concentration for diolein, oleyl alcohol, and lecithin. Lecithin created a surface pressure at low concentrations with a corresponding (π, Γ_0) -curve that was close to linear; a least-squares fit gave a slope of

$$\frac{d\pi}{d\Gamma_0} = 13.6 \quad (0.60 \leq \Gamma_0 < 3.55 \mu\text{g cm}^{-2}). \quad (17)$$

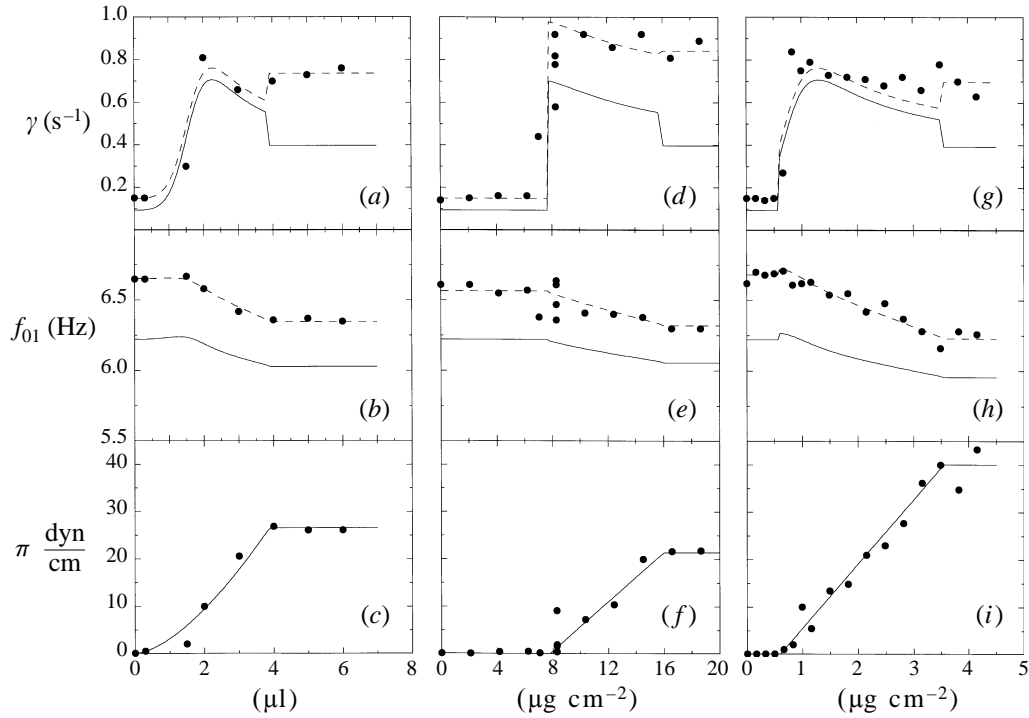


FIGURE 3. ●, measurements, and predictions (—, without and ---, with empirically fit contact-line effects) of the damping rates (*a, d, g*) and natural frequencies (*b, e, h*) of the (0, 1) mode on an air–water interface that is covered with varying concentrations of diolein (*a–c*), oleyl alcohol (*d–f*), and lecithin (*g–i*). (*c*), (*f*) and (*i*) show the measured values of ●, surface pressure, and —, curves from a least-square fit. (The fit is given in the text.)

For $\Gamma_0 < 0.60$ the surface did not feel a surface pressure; for $\Gamma_0 \geq 3.55$ the surface was saturated and additional quantities of lecithin no longer spread or changed the surface pressure. Similarly, a least-squares fit gave the slope of the (π, Γ_0) -curve for oleyl alcohol to be

$$\frac{d\pi}{d\Gamma_0} = 2.6 \quad (7.78 \leq \Gamma_0 < 16.00 \mu\text{g cm}^{-2}), \quad (18)$$

where, for $\Gamma_0 < 7.78$ the surface did not feel a surface pressure and for $\Gamma_0 \geq 16$ the surface was saturated. A linear fit to the (π, Γ_0) -curve was inadequate for the diolein data; a power-law fit provided a gradient of

$$\frac{d\pi}{d\Gamma_0} = 5.0 \Gamma_0^{0.56} \quad (0 \leq \Gamma_0 < 3.88 \mu\text{l}), \quad (19)$$

where for $\Gamma_0 \geq 3.88$ the surface was saturated.

4.2 Damping rates

Figures 3(*a*), 3(*d*), and 3(*g*) show measurements and predictions of damping rates as a function of surfactant concentration for lecithin, oleyl alcohol, and diolein. The discrepancy between predicted and measured damping rates for waves on a clean surface are fairly small relative to the large increase in damping rates due to the presence of surfactants. (We note that damping due to dissipation in the interior has

been shown to be important by Martel, Nicolás & Vega (1998) for experiments using a clean surface and a pinned contact line, but here it is not: the theoretical damping rate for a clean surface without/with the interior damping is $0.0929/0.0933 \text{ s}^{-1}$. Nevertheless, the predicted damping rates were as much as 15% less than those measured on a clean surface. These discrepancies are probably due to the dynamics of the contact line. The dashed curves in figures 3(a), 3(d), and 3(g) show the damping predictions that incorporate contact line dynamics using an empirical value for contact-line speed. They are discussed in §4.4.

In all three experiments the damping rate increased by almost a factor of 10 at very low surfactant concentrations. The theory adequately predicts the concentration at which this jump occurred. For lecithin and diolein, the theory predicted the magnitude of the jump; however, it underpredicted the magnitude for oleyl alcohol. It is possible that the linear fit is inadequate at the sudden jump in surface pressure at about $\Gamma_0 \sim 8 \mu\text{g cm}^{-1}$. In all three experiments the theoretical prediction of damping rate decreased slightly after the initial jump. This decrease is not evident in the data because of too much scatter.

For these three experiments, the model of damping that assumes an inextensible surface (11) is inadequate even when the surface is saturated. When the surface is saturated, the elasticity is zero (rather than infinite as in the inextensible model), so one might expect the waves to damp as if the surface were clean with a reduced value of surface tension. Nevertheless, the waves damped with rates significantly larger than both the clean surface and inextensible surface models predict. Presumably, neither model applies in the saturated regime because during wave passage, the spacing between surfactant molecules increases and decreases providing a finite surface elasticity that enhances damping. This effect would be amplitude-dependent and is not included in the model. However, even when additional surfactant is added, so that the surface is still saturated during wave passage, the damping rate remains about what it is at the point of saturation. This result for insoluble surfactants is in agreement with that of Henderson & Miles (1990), who found that the damping rates of standing waves on water saturated with a soluble detergent were larger than predicted by the inextensible surface model. We note that the discrepancy between measured damping rates and those predicted by the inextensible surface model are greatly in excess of the 15% discrepancy for clean surface waves. A possible explanation is the enhanced damping observed by Huhnerfuss *et al.* (1985*b*) that was due to the relaxation time of the surfactant molecules. Another possible explanation is damping due to contact-line motion as discussed in §4.4 and shown by the dashed curves in figures 3(a, d, g).

4.3. Natural frequencies

Measurements and predictions of natural frequencies are shown in figures 3(b), 3(e), and 3(h). The measured frequencies were always higher than predicted by the viscous, linear dispersion relation, (13), by a fairly constant amount, about 0.30–0.35 Hz, although the variation in frequencies is qualitatively consistent with the predictions. Table 1 lists three sets of values for each correction term in (13) for three surfactants, as well as the contribution to damping from (9). The three sets of values correspond to one point each in the three regimes of the experiments: the clean surface, the elastic surface and the saturated surface. The contributions from the lateral boundaries are negligible, while those of the surface elasticity are almost so. The significant contribution is simply the change in surface tension due to the surfactant films. Thus, the effect of an increasing concentration of surfactant was to decrease the natural frequencies, since the surface tension decreases with increasing concentration. We note

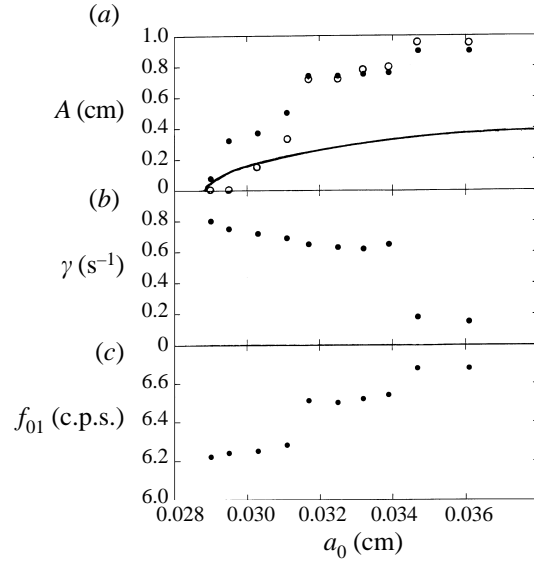


FIGURE 4. Measurements and predictions of (a) wave amplitudes, (b) measured damping rates and (c) measured natural frequencies when the air–water interface was saturated with cholesterol. The solid symbols in (a) are the measurements. The curve is a theoretical prediction that assumes theoretical values for natural frequencies and damping rates. The open symbols correspond to theoretical predictions that incorporate the measured natural frequencies and damping rates.

	Clean	Elastic	Saturated
Diolain			
π (dyn cm ⁻¹)	0	15.2	26.6
ω_{lm} (s ⁻¹)	$6.23 \times 2\pi$	$6.15 \times 2\pi$	$6.09 \times 2\pi$
γ_b (s ⁻¹)	4.84×10^{-3}	4.81×10^{-3}	4.79×10^{-3}
γ_{sw} (s ⁻¹)	8.81×10^{-2}	8.75×10^{-2}	8.70×10^{-2}
γ_e (s ⁻¹)	0	0.145	0
γ_s (s ⁻¹)	0	0.576	γ_s^{in} (s ⁻¹) = 0.305
Oleyl alcohol			
π (dyn cm ⁻¹)	0	15.1	21.4
ω_{lm} (s ⁻¹)	$6.23 \times 2\pi$	$6.15 \times 2\pi$	$6.12 \times 2\pi$
γ_b (s ⁻¹)	4.84×10^{-3}	4.81×10^{-3}	4.80×10^{-3}
γ_{sw} (s ⁻¹)	8.81×10^{-2}	8.75×10^{-2}	8.73×10^{-2}
γ_e (s ⁻¹)	0	0.244	0
γ_s (s ⁻¹)	0	0.491	γ_s^{in} (s ⁻¹) = 0.306
Lecithin			
π (dyn cm ⁻¹)	0	15.0	40.1
ω_{lm} (s ⁻¹)	$6.23 \times 2\pi$	$6.15 \times 2\pi$	$6.02 \times 2\pi$
γ_b (s ⁻¹)	4.84×10^{-3}	4.81×10^{-3}	4.76×10^{-3}
γ_{sw} (s ⁻¹)	8.81×10^{-2}	8.75×10^{-2}	8.65×10^{-2}
γ_e (s ⁻¹)	0	0.135	0
γ_s (s ⁻¹)	0	0.581	γ_s^{in} (s ⁻¹) = 0.303

TABLE 1. Values of the four terms used to calculate natural frequencies from (13) and the contribution to damping due to an elastic surface (γ_s) from (9) at the corresponding surface pressures for the three regimes of experiments using diolain, oleyl alcohol and lecithin surfactants.

that the measurements of the natural frequencies of waves on films that were not concentrated enough to exert a surface pressure did vary slightly with each surfactant, indicating that even a small amount of contamination changes the properties of the contact line.

As shown in table 1, the variation of natural frequency due to elasticity, γ_e , is less than about 1% of the total value, so the elasticity of the film cannot explain the deviation between measured and predicted frequencies. A probable mechanism for the discrepancy is contact-line dynamics. The dashed curves in figures 3(b), 3(e), and 3(h) show the frequency predictions that incorporate contact line dynamics using an empirical value for contact-line speed. This correction is discussed in §4.4.

Another possible explanation for the larger than predicted natural frequencies is dispersion due to finite amplitude. According to Wehausen & Laitone (1960, p. 665), the quadratic-order correction to the dispersion relation for standing, gravity waves on deep water acts to decrease the natural frequency. Tadjbakhsh & Keller (1960) showed that at some critical water depth, the frequency correction acts to increase the natural frequency. The experiments of Fultz (1962) showed that the amplitude correction to the natural frequency of finite-amplitude, standing, gravity waves does change sign at some critical depth; however, his depth was about 20% less than predicted. Concus (1962) calculated the amplitude correction for one (horizontal) dimension, standing, gravity-capillary waves on finite depth and mapped out a depth *vs.* surface tension space that showed regions for which the frequency correction was either positive or negative. A quadratic order amplitude correction is valid when waves have small amplitude. However, numerical calculations of steep standing waves (e.g. Vanden-Broeck & Schwartz 1981, Mercer & Roberts 1992) show that the frequency of limiting-form standing waves does not vary monotonically with amplitude. Their calculations are for one (surface)-dimensional waves in a rectangular geometry. Our measurements for wave frequencies do not fit into any of these investigations; the waves are one (surface)-dimensional because they are axisymmetric, however, they are created in a circular geometry.

We do not believe that amplitude dispersion is the cause for the larger than predicted natural frequencies as explained below. Nevertheless, there is evidence in our experiments that amplitude effects on frequencies are present (amplitude effects in general are discussed in more detail in §4.5). Figure 4 shows measurements of wave amplitudes and natural frequencies (as well as damping rates, which are discussed in §4.5) for waves on an air-water interface that was saturated with a cholesterol film. There is a strong correlation between increasing wave amplitude and increasing natural frequency. We believe that this correlation is the result of wetting properties along the cylinder walls, rather than amplitude dispersion. In particular, consider figure 2, which shows data for a large amplitude wave and evidence of amplitude dispersion for small times after the forcing is removed. In this experiment, during forcing, $Ak_{01} \sim 1$. Immediately after the forcing was stopped (about $2 < t < 3$), the damping rate had a constant value (figure 2b), while the frequency (figure 2c) varied with the decaying wave amplitude. Thus, figure 3(c) shows that when the amplitude was large (about $2 < t < 3$), the frequency was a function of amplitude. When the wave slope decreased to about 0.4, the decay rate changed to a different, constant value, and the frequency maintained a constant value, which was the one measured and reported. Thus, for a smaller wave amplitude, the frequency was not amplitude dependent.

In sum, figure 2 shows that frequencies depended on the amplitude of the wave just after the forcing was stopped. However, the measurements of natural frequencies were obtained during the latter part of the wave decay, when the frequencies were not

	Clean	Elastic	Saturated
Diiolein			
π (dyn cm ⁻¹)	0	0	3.10
$\lambda_R \omega l_c$ (cm s ⁻¹)	0.32	0.32	1.96
$\lambda_I \omega l_c$ (cm s ⁻¹)	4.52	4.52	4.27
$ \lambda \omega l_c$ (cm s ⁻¹)	4.53	4.53	4.70
$\arctan(\lambda_R/\lambda_I)$	1.50	1.50	1.14
Oleyl alcohol			
π (dyn cm ⁻¹)	0	7.78	16.00
$\lambda_R \omega l_c$ (cm s ⁻¹)	0.50	2.47	3.91
$\lambda_I \omega l_c$ (cm s ⁻¹)	8.51	8.21	7.71
$ \lambda \omega l_c$ (cm s ⁻¹)	8.53	8.57	8.65
$\arctan(\lambda_R/\lambda_I)$	1.51	1.28	1.10
Lecithin			
π (dyn cm ⁻¹)	0	0.60	3.55
$\lambda_R \omega l_c$ (cm s ⁻¹)	0.28	0.28	1.55
$\lambda_I \omega l_c$ (cm s ⁻¹)	3.52	3.52	3.36
$ \lambda \omega l_c$ (cm s ⁻¹)	3.53	3.53	3.70
$\arctan(\lambda_R/\lambda_I)$	1.49	1.49	1.14

TABLE 2. Empirical values for the real and imaginary parts, magnitudes and phases of the contact-line speed at the corresponding surface pressures for the three regimes of experiments using diiolein, oleyl alcohol and lecithin surfactants.

amplitude dependent. Thus, the discrepancy between measured frequencies and predictions cannot be explained using a quadratic order correction to the dispersion relation.

4.4. Contact line effects

Previous investigations (see, e.g. Cociaro, Faetti & Festa 1993, Henderson *et al.* 1992) showed that damping rates can be significantly increased due to contact line dynamics and acute contact angles. Cocciario *et al.* (1993) further showed that when wave amplitudes were small, but not small enough so that the contact line was pinned, the natural frequencies and damping rates were affected by contact-line dynamics. When the amplitudes were large, the natural frequency and damping rate were not affected by contact-line dynamics. Here, the amplitudes of the waves are large during and just after forcing, but the damping rates and natural frequencies were measured during the time period in which the amplitudes became small. We have no quantitative measurements of the contact angle or the contact-line speeds. Visually, it appeared that the static contact angle did not change with the addition of surfactant; however, this statement is a very qualitative one.

To incorporate the effects of the contact line into the predictions of damping rates and natural frequencies, we use Miles' (1991) results, written herein as equations (14)–(16). Since we do not have measurements of the contact-line speed, $c = \omega l_c (\lambda_R + i\lambda_I)$, we chose three values for λ_R and λ_I for each surfactant. These values are presented in table 2. The three values correspond to the three regimes of experiments using one surfactant: the regime in which the surfaces were clean, elastic and saturated. The values for λ , which are used in the predictions, vary throughout each regime with surface pressure, so only the initial surface pressure of each regime and the corresponding value of λ are listed.

The values of λ_R and λ_I were chosen such that the real part of (16) is constant for

experiments using a particular surfactant, except for the scale factor of the capillary length l_c , which changes with surface pressure. As a result, the contact-line speed for waves on oleyl alcohol is about twice those on diolein and lecithin. The imaginary part of (16) may change markedly for each regime to account for the varying differences between predictions and measurements of damping rates in the three regimes of each set of experiments. In general, the dashed curves in figure 3(*a, d, g*) correspond to (6) plus the imaginary part of (16). The dashed curves in figure 3(*b, e, h*) correspond to (13), with ω_{lm} replaced by the real part of (16).

If we accept this empirical fit to be valid, then table 2 shows that the magnitude of the contact-line speed increased slightly with increasing surfactant, but only by about 1% when oleyl alcohol was used and 4 or 5% when diolein and lecithin were used. However the phase changed by about 10%. When the surface was clean, the phase was about $\frac{1}{2}\pi$. The 'clean' regime is defined to be the regime where surfactant was added but the surface did not feel a surface pressure, and the damping rates corresponded to those of a clean surface. However, the measured natural frequencies did change a small amount in this regime, even though no surface pressure was felt, particularly when lecithin was used. Thus, even when the amount of contamination is too small to effect damping rates, it is enough to affect natural frequencies a small amount by changing the contact-line speed.

We note that the values for wave speed obtained empirically herein are consistent with measurements by Ting & Perlin (1995). They measured the speed of the contact line on an oscillating glass plate in water. A 6 Hz, 3 mm (amplitude) oscillation produced a contact-line speed of 3.6 cm s^{-1} (this value was obtained by estimation from their figure 10). If the contact-line had moved with the plate, its speed would have been roughly 7 cm s^{-1} . Here, the wave amplitudes during forcing were about 1 cm; however, damping rates and natural frequencies were measured after the amplitudes had decreased to a value starting around 0.4 cm (see figure 2*a*). Thus, our empirical values for contact-line speed are comparable to their measured values, although they were considering water on a flat, vertical plate, while we have water with surfactant films on a curved plate.

4.5. Wave amplitudes

Wave amplitudes had a profound effect on the damping rates in experiments using arachidyl alcohol and cholesterol. Figure 5 shows the measurements of damping rates and surface pressures as a function of concentration of arachidyl alcohol. The (π, Γ_0) -curve shows that indeed, the surface felt large pressures; nevertheless, the damping rate remained about what it was for a pure surface and seemed independent of the surface pressure. When the surface was saturated with cholesterol, the waves also damped as if the surface was clean. We investigated and ruled out a number of possible experimental causes for this result, but finally determined that the small damping rates were due to the large amplitudes of the waves. Figure 4 shows measurements of damping rates of waves on a surface saturated with cholesterol when the forcing amplitude of the motor, and consequently the wave amplitude was increased. These data show that when the wave amplitudes were large (the slopes approached 1), they damped as if there were no surfactant present. Recall, that for these experiments, the surface was saturated with cholesterol, so the surface tension was the same for each experiment depicted in figure 4. This large-amplitude effect was only true for the arachidyl alcohol and cholesterol surfactants. It did not occur for lecithin, oleyl alcohol and diolein. A calculation of the surface pressure based on the area of the strained surface does not support the conjecture that the elasticity had changed significantly to be negligible in its effect on damping. A possible explanation is that the arachidyl

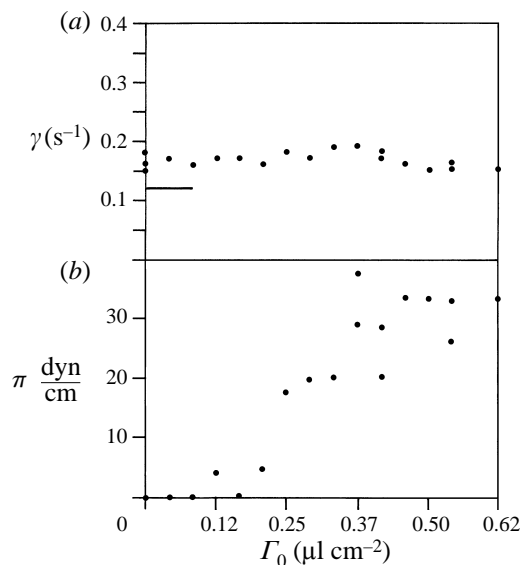


FIGURE 5. Measurements of (a) damping rates and (b) surface pressures for an interface with varying concentrations of arachidyl alcohol. The solid line in (a) is the theoretical damping rate when the surface is clean.

alcohol and cholesterol monolayers do not remain intact for highly strained surfaces; however, we do not have a method to test this.

Another possible explanation for the difference between damping results for the oleyl alcohol, lecithin, and diolein films, which produced damping rates that increased with increasing concentration as expected, and with those of arachidyl alcohol and cholesterol, which did not, is the solid or liquid state of the film created by the surfactants. The first three surfactants create liquid films, while arachidyl alcohol creates a more rigid, solid film. However, Henderson (1990) examined damping rates on mixtures of solid/liquid films, using varying percentages of arachidyl alcohol/cholesterol and cholesterol/lecithin surfactants. Previous measurements of evaporation (Rao & Shah 1990) showed that at a critical ratio of solid/liquid surfactant, the behaviour of the film changed from solid to liquid (with regard to how much of the bulk fluid was able to evaporate through the film). This change in state of the film did not manifest itself in the damping rates. Y. K. Rao (private communication) provides the following possible explanation for the damping behaviour using cholesterol films. Cholesterol molecules are like a book in that when they are not compressed, they may open up, consuming space and exerting a large surface pressure. When they are compressed, they fold so that the film is not saturated. Thus, when the surface was quiescent, the molecules exerted the measured surface pressure, but during wave passage, they may have exhibited the folding behaviour so that the surface no longer felt the pressure and the waves damped as though the surface felt no pressure.

Figure 4 also shows the prediction of wave amplitudes from Henderson & Miles (1990) that considers only the change in surface tension due to the surfactant. They showed that this theory does a good job in predicting wave amplitudes for the (0, 1) mode. They used a wetting agent that minimized contact line effects. The solid curve shows the predictions using predicted natural frequencies and damping coefficients. It grossly underpredicts the measured amplitudes. The hollow circles show predictions using the measured natural frequencies and measured damping rates that are shown in

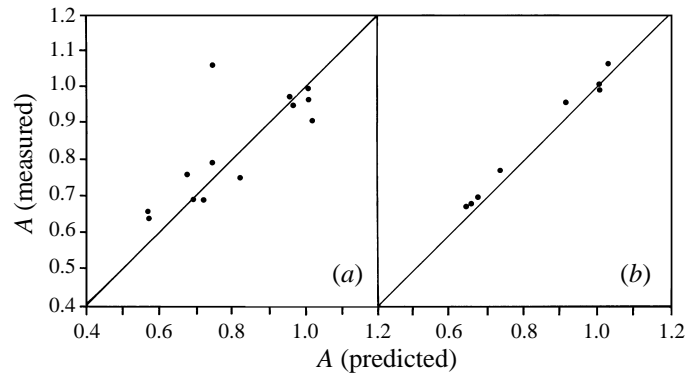


FIGURE 6. Measured *vs.* predicted wave amplitudes for waves on a surface with varying concentrations of (a) oleyl alcohol and (b) diolein. Predictions use measured values of damping rates and natural frequencies. The amplitudes are normalized by the measured amplitude on the corresponding clean surface.

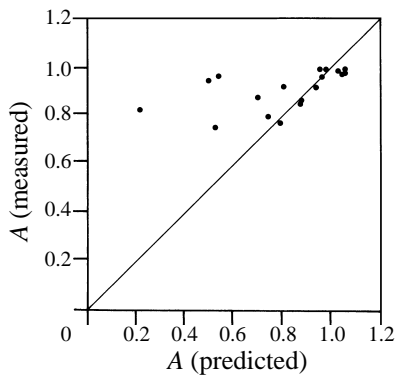


FIGURE 7. Measured *vs.* predicted wave amplitudes for waves on a surface with varying concentrations of lecithin. Predictions use measured values of damping rates and natural frequencies. The amplitudes are normalized by the measured amplitude on the corresponding clean surface.

figures 4(b) and 4(c). These predictions are in fair agreement for the large-amplitude waves. This agreement is actually somewhat remarkable, since the theory assumes small wave slopes, which are larger than one in some experiments. Surprisingly, the agreement is very poor for small-amplitude waves. In fact, for the first two experiments the theory predicted that the quiescent surface should remain stable. This result is probably due to contact line effects, which, as discussed earlier, are more significant for small-amplitude waves.

We note that for most of the experiments with arachidyl alcohol the wave amplitudes changed very little or increased slightly with the presence of surfactant as compared to the clean-surface amplitudes. This result is in marked contrast to the wave amplitudes of the waves on oleyl alcohol and diolein. The measured amplitudes of waves on these films, normalized by the clean surface value, are shown in figure 6 as a function of predicted (normalized) amplitudes. Predictions are made by incorporating measured values of surface tension, damping rate and natural frequency. For waves on oleyl alcohol and diolein, the predictions are in fairly good agreement with measurements. In particular, wave amplitudes decreased with decreasing surface tension. The amplitudes of waves on a lecithin film, shown in figure 7, decreased only slightly with decreasing surface tension. This result is similar to that observed for wave amplitudes

on arachidyl alcohol films; wave amplitudes did not decrease significantly with decreasing surface tension. However, the damping rates of waves on lecithin were in reasonable agreement with predictions, while those for waves on arachidyl alcohol were not.

We note that one difference between the films created by arachidyl alcohol and lecithin are that the former are solid-like and the latter are liquid-like. However, the state of the film does not provide an explanation for either the amplitude behaviour or the damping behaviour. In particular, the damping behaviour of waves was peculiar using films of arachidyl alcohol and cholesterol, the first of which creates a solid film, the second of which creates a liquid film. The amplitude behaviour was peculiar using films of arachidyl alcohol and lecithin, the first of which creates a solid film, the second of which creates a liquid film. Thus, the state of the film does not seem to be a dominant feature in the experiments, since both types of films exhibited peculiar behaviour for both damping results and amplitude results.

5. Summary and conclusions

We examined the damping rates, natural frequencies and wave amplitudes of waves on a water surface that was contaminated with varying concentrations of surfactants. Five surfactants were used; (i) oleyl alcohol, (ii) lecithin, (iii) diolein, (iv) arachidyl alcohol, and (v) cholesterol. We found the following results:

1. Measured damping rates of waves were in reasonable agreement with predictions of Miles (1967), which include surface elasticity, in experiments using films (i), (ii) and (iii). Discrepancies may be accounted for by considering excess damping due to the contact-line dynamics.

2. When the surface was saturated with surfactant, the damping rates were greatly in excess of both the clean surface model and inextensible surface model predictions, indicating that although the quiescent surface had zero elasticity, during wave passage the surface had a finite elasticity.

3. Measured damping rates were unaffected by surfactants (iv) and (v) when the wave amplitudes were large.

4. Measured natural frequencies were larger than predicted in all experiments but were in qualitative agreement with predictions when the dispersion relation included viscous and elastic effects. The inclusion of contact-line effects in the calculations increases the predicted value of natural frequency. Thus, an empirical value for contact-line speed is obtainable that causes predictions and measurements to agree. This result shows that Miles' (1991) approach in allowing the contact-line speed to be complex in the boundary condition at the lateral boundary is necessary to model effects on both the wave damping and the natural frequencies.

5. Measured amplitudes were in reasonable agreement with weakly nonlinear predictions that used measured values of natural frequencies and damping rates, for experiments using films (i), (iii) and (v). Predictions included only the change in surface tension owing to the films; it did not include the elasticity of the film.

6. Measured amplitudes did not agree with predictions for experiments using films (ii) and (iv); with these films, the wave amplitudes changed only slightly with increasing surfactant concentration. Further, with (iv) the wave amplitudes increased slightly with decreasing surface tension, in contrast to theoretical predictions.

The author is grateful to Joe Hammack, who helped design the experimental apparatus, to Joe Hammack and Dinesh Shah for useful discussions, to Pramod

Kumar who prepared the surfactants and spread them on the air–water interface, to the University of Florida where these experiments were conducted, and to the referees.

REFERENCES

- ADAMSON, A. W. 1990 *Physical Chemistry of Surfaces*. Wiley.
- ALPERS, W. & HUHNERFUSS, H. 1989 The damping of ocean waves by surface films: A new look at an old problem. *J. Geophys. Res.* **94**, 6251–6265.
- BOCK, E. J. 1987 On ripple dynamics I. Microcomputer-aided measurement of ripple propagation. *J. Colloid Interface Sci.* **119**, 326–333.
- BOCK, E. J. 1989 On ripple dynamics IV. Linear propagation of plane-wave packets: Observation. *J. Colloid Interface Sci.* **131**, 38–46.
- BOCK, E. J. & MANN, A. 1989 On ripple dynamics II. A corrected dispersion relation for surface waves in the presence of surface elasticity. *J. Colloid Interface Sci.* **129**, 501–505.
- CASE, K. M. & PARKINSON, W. X. 1957 Damping of surface waves in an incompressible liquid. *J. Fluid Mech.* **2**, 172–184.
- CINI, R. & LOMBARDINI, P. P. 1978 Damping effect of monolayers on surface wave motion in a liquid. *J. Colloid Interface Sci.* **65**, 387–389.
- CINI, R. & LOMBARDINI, P. P. 1981 Experimental evidence of a maximum in the frequency domain of the ratio of ripple attenuation in monolayered water to that in pure water. *J. Colloid Interface Sci.* **81**, 125–131.
- COCCIARO, B., FAETTI, S. & FESTA, C. 1993 Experimental investigation of capillarity effects on surface gravity waves: non-wetting boundary conditions. *J. Fluid Mech.* **246**, 43–66.
- CONCUS, P. 1962 Standing capillary–gravity waves of finite amplitude. *J. Fluid Mech.* **14**, 568–576.
- DAVIES, J. T. & VOSE, R. W. 1965 On the damping of capillary waves by surface films. *Proc. R. Soc. Lond. A* **260**, 218–233.
- FULTZ, D. 1962 An experimental note on finite-amplitude standing gravity waves. *J. Fluid Mech.* **13**, 193–212.
- HAMMACK, J. L. & HENDERSON, D. M. 1993 Resonant interactions among surface water waves. *Ann. Rev. Fluid Mech.* **25**, 55–97.
- HENDERSON, D. M. 1990 On the damping of Faraday waves. *Proc. Fluid Mechanics and Related Matters, a symposium honoring John Miles on his Seventieth Birthday*. Scripps Institution of Oceanography Reference Series 91–24, pp. 121–131.
- HENDERSON, D., HAMMACK, J., KUMAR, P. & SHAH, D. 1992 The effects of static contact angles on standing waves. *Phys. Fluids A* **4**, 2320–2322.
- HENDERSON, D. M. & MILES, J. W. 1990 Single-mode Faraday waves in small cylinders. *J. Fluid Mech.* **213**, 95–109.
- HOCKING, L. M. 1987 The damping of capillary–gravity waves at a rigid boundary. *J. Fluid Mech.* **179**, 253–266.
- HUHNERFUSS, H., LANGE, P. & WALTER, W. 1985*a* Relaxation effects in monolayers and their contribution to water wave damping I. Wave-induced phase shifts. *J. Colloid Interface Sci.* **108**, 430–441.
- HUHNERFUSS, H., LANGE, P. & WALTER, W. 1985*b* Relaxation effects in monolayers and their contribution to water wave damping II. The Marangoni phenomenon and gravity wave attenuation. *J. Colloid Interface Sci.* **108**, 442–450.
- KEULEGAN, G. H. 1959 Energy dissipation in standing waves in rectangular basins. *J. Fluid Mech.* **6**, 33–50.
- LAMB, H. 1895 *Hydrodynamics*, 2nd edn, §304, p. 552. Cambridge University Press.
- LAMB, H. 1945 *Hydrodynamics*, 6th edn, §257, p. 440. Dover.
- LUCASSEN, J. 1982 Effect of surface-active material on the damping of gravity waves: A reappraisal. *J. Colloid Interface Sci.* **85**, 52–58.
- LUCASSEN, J. & HANSEN, R. S. 1965 *J. Colloid Interface Sci.* **22**, 319.
- LUCASSEN–REYNDERS, E. H. & LUCASSEN, J. 1969 Properties of capillary waves. *Adv. Colloid Interface Sci.* **2**, 347–395.

- MARTEL, C., NICOLÁS, J. A. & VEGA, J. M. 1998 Surface-wave damping in a brimful circular cylinder. *J. Fluid Mech.* **360**, 213–228.
- MERCER, G. N. & ROBERTS, A. J. 1992 Standing waves in deep water: their stability and extreme form. *Phys. Fluids A* **4**, 259–269.
- MILES, J. W. 1967 Surface-wave damping in closed basins. *Proc. R. Soc. Lond. A* **297**, 459–75.
- MILES, J. W. 1984 Nonlinear Faraday resonance. *J. Fluid Mech.* **146**, 285–302.
- MILES, J. W. 1991 The capillary boundary layer for standing waves. *J. Fluid Mech.* **222**, 197–205.
- MILES, J. & HENDERSON, D. 1990 Parametrically forced surface waves. *Ann. Rev. Fluid Mech.* **22**, 143–65.
- PERLIN, M., HENDERSON, D. & HAMMACK, J. 1990 Experiments on ripple instabilities. Part 2. Selective amplification of resonant triads. *J. Fluid Mech.* **219**, 51–80.
- PERLIN, M. & HAMMACK, J. 1991 Experiments on ripple instabilities. Part 3. Resonant quartets of the Benjamin–Feir type. *J. Fluid Mech.* **229**, 229–268.
- PERLIN, M. & TING, C.-L. 1992 Steep gravity–capillary waves within the internal resonance regime. *Phys. Fluids A* **4**, 2466–2478.
- RAO, Y. K. & SHAH, D. O. 1990 Detection of phase transitions in monolayers using retardation of evaporation of water. *J. Colloid Interface Sci.* **137**, 25–29.
- SCOTT, J. C. 1989 Oil slicks still the waves. *Nature* **340**, 601–602.
- TADJBAKHSI, I. & KELLER, J. B. 1960 Standing surface waves of finite amplitude. *J. Fluid Mech.* **8**, 442–51.
- TING, C.-L. & PERLIN, M. 1995 Boundary conditions in the vicinity of the contact line at a vertically oscillating upright plate: an experimental investigation. *J. Fluid Mech.* **295**, 263–300.
- VANDEN-BROECK, J.-M. & SCHWARTZ, L. W. 1981 Numerical calculation of standing waves in water of arbitrary uniform depth. *Phys. Fluids A* **24**, 812–815.
- WEHAUSEN, J. V. & LAITONE, E. V. 1960 *Handbuch der Physik* (ed. S. F. Flugge), vol. 2. Springer.